

# UC Davis

## UC Davis Previously Published Works

### Title

Fission Yeast TORC1 Promotes Cell Proliferation through Sfp1, a Transcription Factor Involved in Ribosome Biogenesis.

### Permalink

<https://escholarship.org/uc/item/45g283c3>

### Journal

Molecular and Cellular Biology, 43(12)

### Authors

Tai, Yen

Fukuda, Tomoyuki

Morozumi, Yuichi

et al.

### Publication Date

2023

### DOI

10.1080/10985549.2023.2282349

Peer reviewed



RESEARCH ARTICLE

# Fission Yeast TORC1 Promotes Cell Proliferation through Sfp1, a Transcription Factor Involved in Ribosome Biogenesis

Yen Teng Tai,<sup>a,\*#</sup>  Tomoyuki Fukuda,<sup>b,#</sup> Yuichi Morozumi,<sup>a</sup> Hayato Hirai,<sup>c</sup> Arisa H. Oda,<sup>c</sup>  Yoshiaki Kamada,<sup>d,e</sup>  
Yutaka Akikusa,<sup>a</sup>  Tomotake Kanki,<sup>b</sup> Kunihiro Ohta,<sup>c</sup>  Kazuhiro Shiozaki<sup>a,f</sup>

<sup>a</sup>Division of Biological Science, Nara Institute of Science and Technology, Ikoma, Nara, Japan

<sup>b</sup>Department of Cellular Physiology, Niigata University Graduate School of Medical and Dental Sciences, Niigata, Japan

<sup>c</sup>Department of Life Sciences, Graduate School of Arts and Sciences, The University of Tokyo, Tokyo, Japan

<sup>d</sup>National Institute for Basic Biology, Okazaki, Aichi, Japan

<sup>e</sup>Graduate University for Advanced Studies (SOKENDAI), Hayama, Kanagawa, Japan

<sup>f</sup>Department of Microbiology and Molecular Genetics, University of California, Davis, California, USA

**ABSTRACT** Target of rapamycin complex 1 (TORC1) is activated in response to nutrient availability and growth factors, promoting cellular anabolism and proliferation. To explore the mechanism of TORC1-mediated proliferation control, we performed a genetic screen in fission yeast and identified Sfp1, a zinc-finger transcription factor, as a multicopy suppressor of temperature-sensitive TORC1 mutants. Our observations suggest that TORC1 phosphorylates Sfp1 and protects Sfp1 from proteasomal degradation. Transcription analysis revealed that Sfp1 positively regulates genes involved in ribosome production together with two additional transcription factors, Lfh1/Crf1 and Fhl1. Lfh1 physically interacts with Fhl1, and the nuclear localization of Lfh1 is regulated in response to nutrient levels in a manner dependent on TORC1 and Sfp1. Taken together, our data suggest that the transcriptional regulation of the genes involved in ribosome biosynthesis by Sfp1, Lfh1, and Fhl1 is one of the key pathways through which nutrient-activated TORC1 promotes cell proliferation.

**KEYWORDS** fission yeast, rapamycin, ribosome, Sfp1, TORC1, transcription factor

## INTRODUCTION

The target of rapamycin (TOR), a Ser/Thr protein kinase that belongs to the phosphoinositide 3-kinase (PI3K)-related kinase family, is highly conserved among eukaryotes from yeast to humans.<sup>1</sup> TOR kinase participates in two structurally and functionally distinct protein complexes termed TOR complex 1 (TORC1) and 2 (TORC2). TORC1 controls cell growth, proliferation, and metabolism in response to a variety of cues including nutrient availability, growth factors, and cellular energy, while TORC2 is mainly regulated by growth factors and cellular stress to promote cell survival.<sup>2</sup>

Mammalian TORC1 (mTORC1) is regulated by two types of small GTPases localized to lysosomes, Rheb and Rag. The GTP-loaded form of Rheb activates mTORC1 by directly interacting with mTOR.<sup>3</sup> Rheb is negatively regulated by the TSC complex, which carries GTPase-activating protein (GAP) activity toward Rheb.<sup>4</sup> Growth factors stimulate the PI3K–PDK1–Akt pathway, thereby inducing phosphorylation and inactivation of the TSC complex.<sup>5</sup> Amino acid availability activates mTORC1 through the action of the Rag heterodimer, RagA/B bound to RagC/D, which is anchored to lysosomal membranes by a protein complex called Ragulator.<sup>6–8</sup> The GTP-loaded form of RagA/B binds to mTORC1 and mediates the recruitment of mTORC1 to the lysosomal surface where Rheb activates mTORC1.<sup>7,8</sup> RagA/B is negatively regulated by the GAP complex

© 2023 Taylor & Francis Group, LLC

Supplemental data for this article can be accessed online at <https://doi.org/10.1080/10985549.2023.2282349>.

Address correspondence to Tomoyuki Fukuda, [tfukuda@med.niigata-u.ac.jp](mailto:tfukuda@med.niigata-u.ac.jp).

\*Present address: College of Medicine, Pennsylvania State University, Hershey, Pennsylvania, 17033, USA.

#These authors contributed equally to this work.

Received 28 November 2022

Revised 29 October 2023

Accepted 6 November 2023

GATOR1, which is inhibited by another protein complex called GATOR2 to activate mTORC1 in the presence of amino acids.<sup>9</sup>

It has been found in diverse eukaryotes that TORC1 regulates multiple cellular processes to control cell growth and proliferation. When active, TORC1 stimulates anabolic processes, such as biosynthesis of proteins, lipids, and nucleotides, by phosphorylating its downstream effectors.<sup>1</sup> mTORC1 augments protein translation via its substrates, p70 S6 kinase 1 (S6K1) and the eukaryotic translation initiation factor 4E-binding protein (4E-BP).<sup>10,11</sup> mTORC1 also increases lipid synthesis by activating the sterol responsive element-binding protein (SREBP) transcription factors through Lipin 1.<sup>12</sup> Conversely, mTORC1 inhibits catabolic processes such as autophagic degradation of macromolecules by regulating the core autophagy complex ATG13-ULK1-FIP200.<sup>13,14</sup> The balance between anabolic and catabolic processes is crucial for cellular homeostasis; hence, defective human TORC1 signaling often culminates in metabolic disorders and cancer.<sup>15</sup> To better understand how TORC1 regulates cellular physiology, comprehensive identification of the TORC1 substrates and detailed characterization of the molecular events downstream of TORC1 are necessary.

TORC1 and its upstream regulators including Rheb, TSC, Rag, Ragulator, GATOR1, and GATOR2 are well conserved in the fission yeast *Schizosaccharomyces pombe*, a unicellular model eukaryote.<sup>16,17</sup> Fission yeast has two TOR kinases, Tor1 and Tor2, which form TORC2 and TORC1, respectively.<sup>18,19</sup> As in mammalian cells, fission yeast TORC1 phosphorylates multiple substrates to control diverse cellular processes.<sup>20</sup> Although functional TORC1 is essential for fission yeast viability,<sup>18,21–23</sup> none of the known factors downstream of TORC1 is essential for cell proliferation; for instance, absence of Psk1, a TORC1 substrate orthologous to S6K1, or ablation of the S6K1 phosphorylation sites in the ribosomal S6 protein cause no apparent growth defect.<sup>24,25</sup> In this study, to understand the mechanism by which TORC1 promotes cell proliferation in fission yeast, we explored factors downstream of TORC1. We screened for genes whose overexpression restores proliferation of TORC1-defective mutants, and thereby identified the Sfp1 transcription factor, which plays an important role in the expression of the ribosomal protein (RP) and ribosomal biogenesis (Ribi) genes. Our study has successfully linked the proliferation-promoting function of TORC1 to the control of protein synthesis through ribosome production.

## RESULTS

**The *sfp1*<sup>+</sup> gene is a multicopy suppressor of hypomorphic TORC1 alleles.** To gain insights into the mechanism by which TORC1 controls cell proliferation, we set out to identify factors downstream of TORC1 in the proliferation-controlling pathway. An *S. pombe* genomic library constructed with the multicopy vector pAL<sup>26</sup> was screened for genes whose overexpression suppresses the growth defect of *tor2-13*, a temperature-sensitive (*ts*) mutant of the *tor2*<sup>+</sup> gene that encodes the catalytic subunit of TORC1.<sup>22</sup> The screen isolated a plasmid, pALSK53, which suppressed the *ts* growth phenotype and rapamycin sensitivity of the *tor2-13* mutant (Fig. 1A). We found that the plasmid was also able to complement other *tor2* mutant alleles, such as *tor2-19*<sup>22</sup> and *tor2-287*<sup>18</sup> (Fig. 1A). DNA sequencing analysis revealed that pALSK53 contains the *sfp1*<sup>+</sup> gene (SPAC16.05c), which encodes a hypothetical zinc-finger transcription factor similar to its *Saccharomyces cerevisiae* ortholog (Fig. 1B). We cloned the Sfp1-coding sequence and its promoter region into a multicopy plasmid and confirmed that the *sfp1*<sup>+</sup> gene is capable of suppressing the growth defect and rapamycin sensitivity of *tor2 ts* cells (Fig. 1C). Thus, we conclude that overexpression of Sfp1 can alleviate the proliferation defects caused by compromised TORC1 function. The alleviation was dependent on the zinc finger domains of Sfp1. Truncation of amino acids 84 to 105 or amino acids 293 to 442 of Sfp1, which removes the N-terminal or C-terminal zinc finger domains, resulted in reduced growth defect suppression in the *tor2-287* mutant compared to full-length Sfp1 (Fig. 1D).

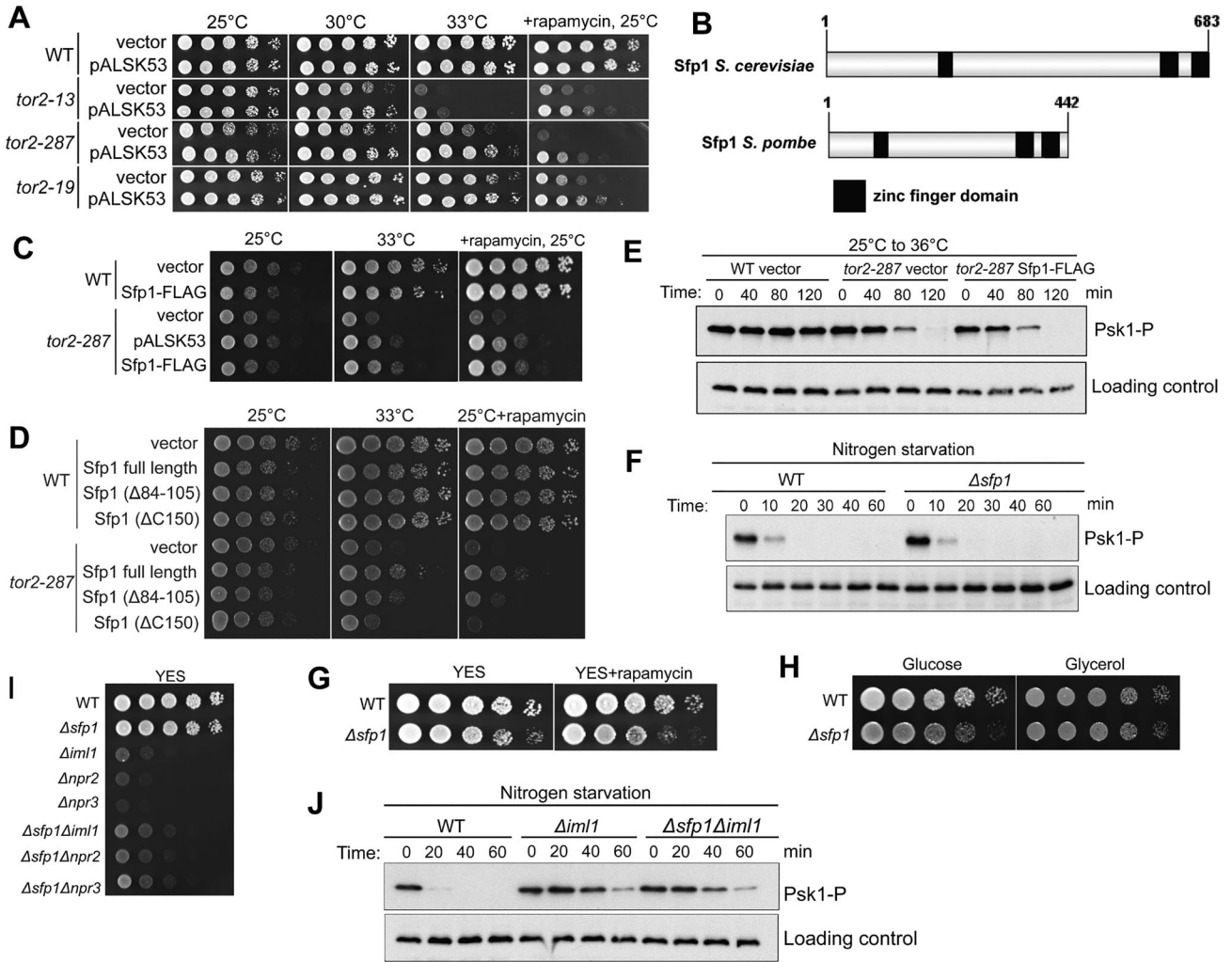


**FIG 1** The *sfp1*<sup>+</sup> gene is a multicopy suppressor of TORC1 hypomorphic alleles. (A) Growth assessment of wild-type (WT) and *tor2* mutant strains carrying the indicated vectors. Serial dilutions of the indicated cells were spotted onto solid EMM medium with or without rapamycin (100 ng/mL), followed by incubation at the specified temperatures. (B) Schematic representation comparing Sfp1 in *S. pombe* and *S. cerevisiae*. (C) Growth assessment of wild-type and *tor2-287* mutant strains carrying either an empty vector, pALSK53, or pSNP-Sfp1-FLAG expressing FLAG-tagged Sfp1 under its native promoter. (D) Growth assessment of wild-type and *tor2-287* mutant strains carrying either an empty vector or pSNP vectors expressing various forms of Sfp1 including the full-length protein and truncated versions with one ( $\Delta 84-105$ ) or two ( $\Delta C150$ ) of the zinc finger domains removed. (E) TORC1 activity in wild-type and *tor2-287* mutant strains carrying either an empty vector or pSNP-Sfp1-FLAG. Cells were cultured in liquid EMM medium at 25°C and shifted to 36°C. TORC1 activity was assessed by detecting TORC1-dependent phosphorylation of Psk1 (Psk1-P). Samples were probed with an anti-Spc1 MAPK antibody as a loading control. (F) TORC1 activity in wild-type and  $\Delta sfp1$  cells was monitored as in (E). Cells were grown in liquid EMM medium and shifted to the same medium without nitrogen. (G and H) Serial dilutions of wild-type and  $\Delta sfp1$  cells were spotted onto solid YES medium with or without 100 ng/mL rapamycin (G) or onto solid medium with 3% glucose or glycerol as the carbon source (H). (I) The indicated strains were spotted in serial dilutions onto solid YES medium. (J) TORC1 activity during nitrogen starvation was monitored in wild-type and indicated mutant strains as described in (F).

We next examined whether overexpression of Sfp1 restores TORC1 activity in the *tor2 ts* mutant. TORC1 activity was monitored by the phosphorylation status of Psk1, a cellular TORC1 substrate.<sup>25</sup> The level of Psk1 phosphorylation was comparable between wild-type and *tor2-287* cells growing at 25°C (Fig. 1E). Upon temperature shift to the restrictive temperature, dephosphorylation of Psk1 was observed with similar kinetics both in the presence and absence of Sfp1 overexpression (Fig. 1E), suggesting that Sfp1 does not affect TORC1 activity. Thus, the complementation of the *tor2* mutant phenotypes by Sfp1 overexpression is not attributed to the restoration of TORC1 activity.

We then constructed a strain whose *sfp1*<sup>+</sup> gene is deleted ( $\Delta sfp1$ ). TORC1 activity monitored by the Psk1 phosphorylation was comparable between wild-type and  $\Delta sfp1$

cells before and after nitrogen starvation (Fig. 1F), further confirming that Sfp1 does not affect TORC1 activity. In contrast, the  $\Delta sfp1$  mutant exhibited a modest growth defect as well as limited rapamycin sensitivity (Fig. 1G), consistent with the notion that Sfp1 is involved in cell proliferation regulated by TORC1. Although the growth defect of the  $\Delta sfp1$  mutant was observed on glucose medium, it grew normally on medium containing glycerol as the carbon source (Fig. 1H), similar to the situation in budding yeast.<sup>27</sup> Notably, the absence of Sfp1 modestly alleviates the growth defect of the mutants lacking functional GATOR1 (Fig. 1I); the absence of GATOR1 causes a severe growth defect due to deregulated TORC1 activation,<sup>28</sup> and therefore, the observed genetic interaction corroborates a functional link between Sfp1 and TORC1. We also confirmed that the  $\Delta sfp1$  mutation did not significantly affect TORC1 activity before and after nitrogen starvation in cells lacking GATOR1 (Fig. 1J). Taken together, these results suggest that Sfp1 controls cell proliferation downstream of, or in parallel with, TORC1.

**TORC1 promotes stable expression of Sfp1.** To determine whether Sfp1 is under regulation by TORC1, we examined the expression pattern of Sfp1 in the presence and absence of TORC1 activity. In the *tor2-287* and *tor2-13* mutants, the Sfp1 protein dramatically decreased within 2 h after shifting to the restrictive temperature (Fig. 2A), suggesting that stable expression of the Sfp1 protein depends on TORC1 activity. Consistently, rapamycin treatment of these *tor2* mutants also caused a severe reduction in the Sfp1 level even at the permissive temperature (Fig. 2B). Conversely, no significant change in the amount of Sfp1 was observed in wild-type cells treated by rapamycin (Fig. 2B), probably because rapamycin does not effectively abolish TORC1 activity and cell proliferation in wild-type fission yeast (Fig. 1A).<sup>28</sup>

To further corroborate that the Sfp1 protein level is regulated by TORC1, we examined the Sfp1 level during nitrogen or glucose starvation, conditions known to inactivate TORC1.<sup>24,25</sup> Sfp1 became undetectable when either of these major nutrients was depleted to suppress TORC1 activity, which was monitored by the Psk1 phosphorylation (Fig. 2C and D); after the growth medium was replenished with the nutrients, the Sfp1 expression was restored along with reactivation of TORC1. Consistent with the immunoblotting analysis, loss of the Sfp1 signal in the nucleus was observed by microscopy (Fig. 2E). In the  $\Delta im11$  mutant lacking the functional GATOR1 complex, both TORC1 inactivation and reduction of Sfp1 were slower than those in the wild-type strain (Fig. 2F). These results show a clear correlation between TORC1 activity and Sfp1 protein levels.

We noticed that, after prolonged nitrogen starvation, the Sfp1 protein level gradually recovered (Fig. 2G), but not during glucose starvation up to 10 h (Fig. 2H). As nitrogen starvation, but not carbon starvation, effectively induces autophagy in fission yeast,<sup>29</sup> we assumed that the recovery of Sfp1 is due to autophagy, which generates nitrogen sources and mitigates TORC1 suppression. To test such a possibility, we utilized the mutants defective in the autophagy induction ( $\Delta atg13$ ) or the autophagic protein degradation in vacuoles ( $\Delta isp6$ ).<sup>30</sup> As expected, the Sfp1 level did not recover in those autophagy-defective mutants even after 6-h starvation of nitrogen (Fig. 2I). We also assessed TORC1 activity by examining the phosphorylation of Psk1 and its target, the S6 protein, confirming that autophagy mitigates TORC1 suppression (Fig. 2J). These observations further emphasize the tight regulation of the Sfp1 protein level by nutrient availability through TORC1 activity.

Although the level of the Sfp1 protein is regulated in response to nutrients, a previous transcriptome analysis indicated that the *sfp1*<sup>+</sup> mRNA level does not change significantly during starvation.<sup>31</sup> Therefore, we hypothesized that the Sfp1 protein is post-translationally regulated through proteasomal degradation. To test this hypothesis, we utilized a *ts* mutant of the 26S proteasome subunit, *mts3-1*, in which the ubiquitin-dependent proteolysis is compromised at the restrictive temperature of 36 °C.<sup>32</sup> After incubation of wild-type and *mts3-1* strains at 36 °C for 2 h, both strains were subjected to nitrogen starvation and the Sfp1 level was monitored by immunoblotting.



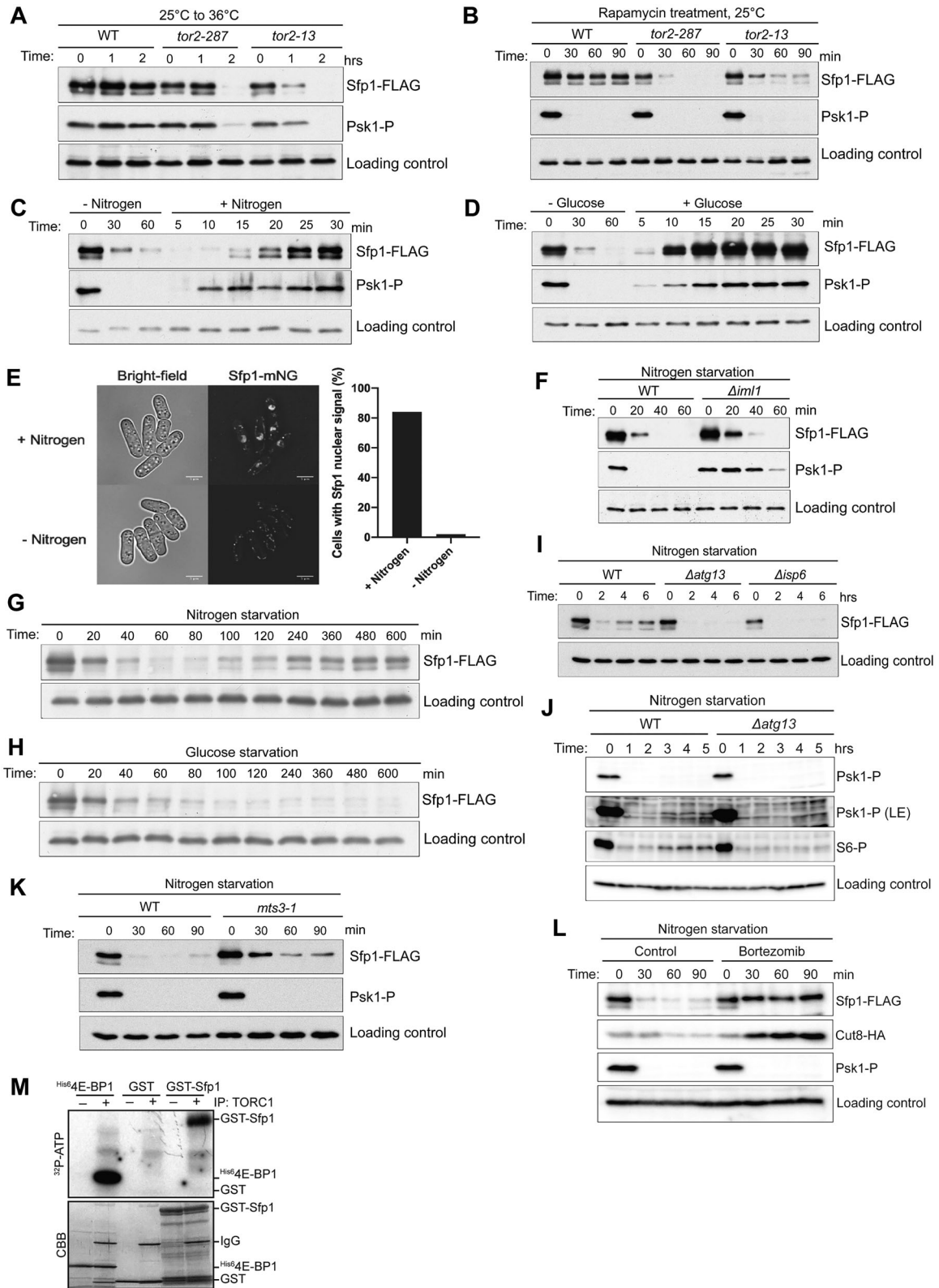


**FIG 2** TORC1 facilitates stable expression of Sfp1. (A) C-terminal FLAG-tagged Sfp1 was expressed from its native chromosomal locus and analyzed by immunoblotting. The indicated strains were grown in liquid YES medium at 25°C and then shifted to 36°C. TORC1 activity was assessed as in Fig. 1E. (B) The indicated strains were grown in liquid YES medium and shifted to the same medium with 200 ng/mL rapamycin. (C and D) Cells expressing Sfp1-FLAG were grown in liquid EMM medium and shifted to the same medium without nitrogen (C) or glucose (D). After 60 min of starvation, ammonium (C) or glucose (D) was added. (E) Cells expressing Sfp1 tagged with C-terminal mNeonGreen (mNG) from its native chromosomal locus were subjected to microscopy analysis. Z-axial images were collected, and mid-section images after deconvolution were shown. The number of cells exhibiting Sfp1 nuclear signal under nitrogen-rich and nitrogen-deficient conditions was quantified. Scale bars, 5 μm. (F) The indicated strains were grown in liquid EMM medium

The reduction of the Sfp1 protein upon nitrogen starvation was significantly delayed in the *mts3-1* mutant (Fig. 2K), suggesting that the stability of Sfp1 during starvation is regulated by the proteasome. This finding was further validated with the proteasome inhibitor bortezomib.<sup>33</sup> In its presence during nitrogen starvation, Sfp1 degradation was impaired (Fig. 2L). Therefore, under nutrient-rich conditions, active TORC1 protects the Sfp1 protein from proteasomal degradation.

Finally, to gain deeper insights into the involvement of TORC1 in regulating Sfp1, we investigated the possibility that TORC1 directly phosphorylates Sfp1. An in vitro kinase assay using Sfp1 as a substrate indicated that Sfp1 is a substrate of TORC1 (Fig. 2M).

**Sfp1 is a transcription factor that regulates genes involved in ribosome production.** The results shown above indicate that nutrient-activated TORC1 positively regulates the Sfp1 transcription factor by stabilizing it. In order to understand the cellular function of the TORC1–Sfp1 pathway, we undertook the identification of the genes whose expression is controlled by the Sfp1 transcription factor. Exponentially growing wild-type and  $\Delta$ *sfp1* cells were subjected to gene expression profiling analysis by the RNA-sequencing (RNA-seq) technique, and the genes with their expression altered by the  $\Delta$ *sfp1* mutation were determined. In comparison with the wild-type strain, 152 genes were upregulated and 318 genes were downregulated in the  $\Delta$ *sfp1* strain. The GO function analysis suggested that the genes downregulated in the  $\Delta$ *sfp1* mutant are implicated in multiple biological functions including RNA helicase activity, RNA binding, and cyclic compound binding. Importantly, apparent enrichment of the ribosome-related GO terms was observed (Fig. 3A).

Ribosome biogenesis requires the expression of the two major classes of genes, the RP genes encoding the ribosome subunits and the Ribi genes encoding the factors that assist rRNA processing and assembly of the ribosome.<sup>34</sup> Our RNA-seq data indicated that among 141 RP and 292 Ribi genes in fission yeast (Supplementary material, Table S1), 31.9% of the RP genes (45 genes) and 26.4% of the Ribi genes (77 genes) are downregulated in the  $\Delta$ *sfp1* mutant (Fig. 3B and C, and Supplementary material, Table S2). Collectively, these results imply that the Sfp1 transcription factor promotes the expression of the genes required for ribosome biosynthesis, a critical process for protein synthesis linked to cell growth.

**Sfp1 functions with the Ifh1-Fhl1 complex in the regulation of ribosome production.** An Sfp1 ortholog in *S. cerevisiae* regulates the expression of the RP genes, together with the forkhead-like transcription factor Fhl1 that interacts with the Ifh1 coactivator and the Crf1 corepressor.<sup>35–37</sup> The genes encoding Ifh1 and Crf1 are derived from the duplication of a single ancestral gene.<sup>38</sup> Fission yeast harbors a single ortholog of Ifh1/Crf1 encoded by SPAC22H10.11c, which we will refer to as Ifh1 hereafter. While fission yeast Ifh1 exhibits limited homology with budding Ifh1/Crf1, multiple sequence alignment analysis predicts the presence of a forkhead-binding domain and the CK2 consensus phosphorylation sites, which are known to be involved in the function of Ifh1/Crf1 in budding yeast (Fig. 4A).<sup>39</sup> Fission yeast also possesses Fhl1 (Fig. 4A), which plays a role in the transcription of nitrogen starvation-responsive genes.<sup>40</sup>

To probe the functional relationship among Sfp1, Ifh1, and Fhl1 in fission yeast, we investigated the genetic interaction among the null mutations of these transcription factors. When compared to wild-type cells, the mutants lacking any one of these

---

#### FIG 2 Legend (Continued)

and shifted to the same medium without nitrogen. (G and H) Sfp1 protein levels during prolonged nitrogen (G) or glucose (H) starvation. (I and J) The indicated strains were grown in liquid EMM medium and shifted to the same medium without nitrogen. LE, long exposure. (K) Wild-type and *mts3-1* cells were incubated at 36 °C for 2 h before nitrogen starvation and analyzed as in (F). (L) Sfp1 protein degradation during nitrogen starvation was monitored in the presence or absence of the proteasome inhibitor bortezomib (1 mM), with the degradation of the proteasome target Cut8 as a control. (M) In vitro TORC1 kinase assay. TORC1 was immunoprecipitated from cells expressing FLAG-tagged Mip1 and incubated with recombinant His<sub>6</sub>4E-BP1, GST, or GST-Sfp1. Phosphorylation and proteins were visualized by autoradiography and Coomassie staining (CBB), respectively.

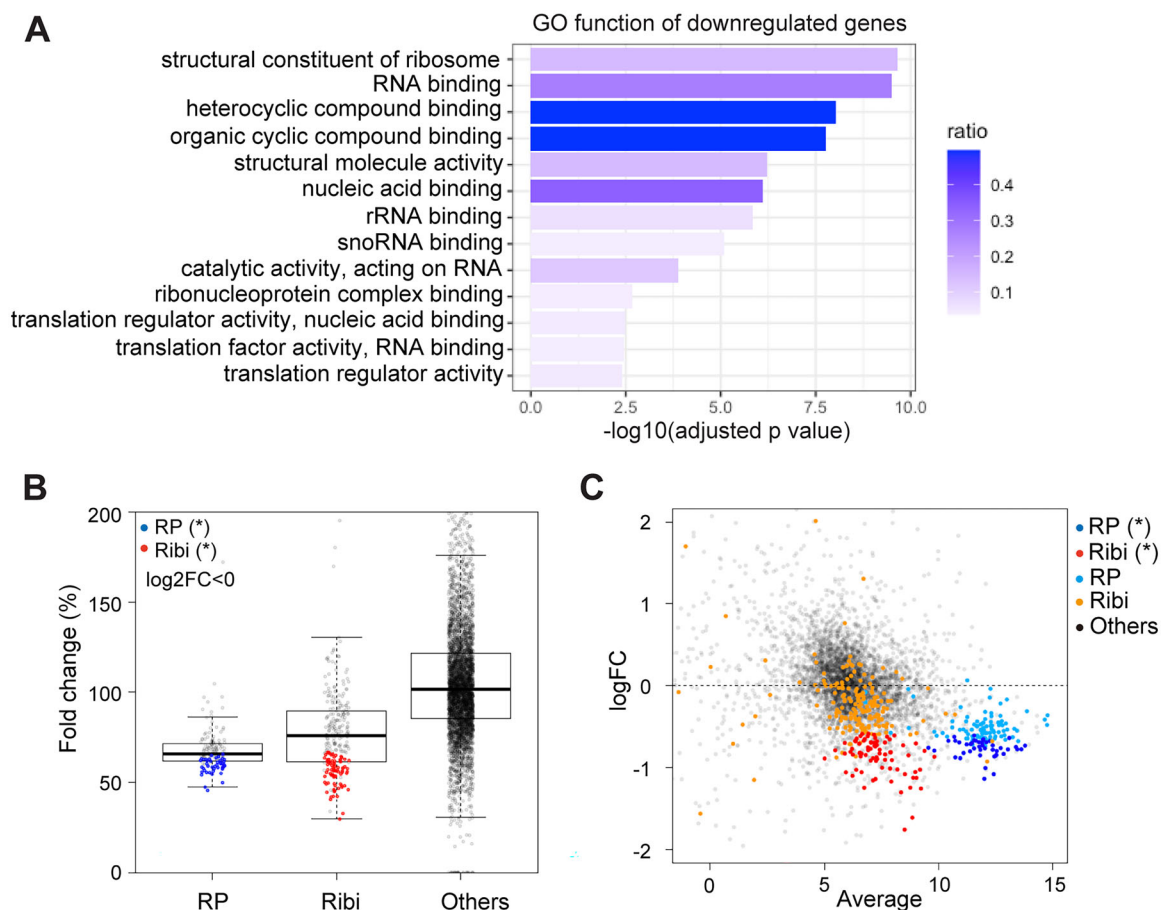


**FIG 3** *Sfp1* is a transcription factor that regulates genes involved in ribosome production. (A) GO functional analysis of genes that are downregulated in the  $\Delta sfp1$  mutant in comparison to the wild-type strain. The x axis (in logarithmic scale) represents adjusted *P* values. Gene ratio is defined as cluster frequency over genome frequency associated with a GO term. (B and C) Box (B) and MA (C) plots depicting the fold change of the downregulated RP ( $n = 141$ ) and Ribi ( $n = 292$ ) genes in the  $\Delta sfp1$  mutant relative to the wild type. Significant differences between the wild type and the mutant are denoted by asterisks ( $P < 0.05$ ).

transcription factors exhibited slow-growth phenotypes, with that of the  $\Delta ifh1$  mutant being the most severe (Fig. 4B). Importantly, no significant additive phenotype was observed when the mutations were combined (Fig. 4B), suggesting that *Sfp1*, *Ifh1*, and *Fhl1* function in the same pathway that regulates cell proliferation. Consistently, like the  $\Delta sfp1$  mutation (Fig. 1I), the  $\Delta ifh1$  and  $\Delta fh11$  mutations were also able to ameliorate the growth defect caused by the absence of the functional GATOR1 complex (Fig. 4C).

We further examined the physical interaction among *Sfp1*, *Ifh1*, and *Fhl1* by co-immunoprecipitation assays. *Ifh1* was co-immunoprecipitated with *Fhl1* both in nutrient-rich and nutrient-starved conditions (Fig. 4D), whereas we currently have not succeeded in detecting the interaction of *Sfp1* with *Ifh1* or *Fhl1* (data not shown). The interaction between *Fhl1* and *Ifh1* was impaired in the mutant expressing *Fhl1* without the N-terminal 150 amino acid residues (Fig. 4E), indicating that the *Ifh1*-*Fhl1* interaction depends on the forkhead-associated (FHA) domain of *Fhl1*. The *Ifh1*-*Fhl1* association was detected both in the presence and absence of *Sfp1*, suggesting that *Sfp1* is not required for their interaction (Fig. 4F). It was found, however, that the amount of the *Ifh1*-*Fhl1* complex was reduced in the  $\Delta sfp1$  mutant when compared to that in the wild-type strain.

To investigate whether *Ifh1* and *Fhl1* are involved in the expression of the genes regulated by *Sfp1*, RNA-seq analyses were carried out with the  $\Delta ifh1$  and  $\Delta fh11$  mutants. In comparison to the wild-type strain, 57 genes were upregulated and 272 genes were downregulated in  $\Delta ifh1$ , while 66 genes were upregulated and 101 genes



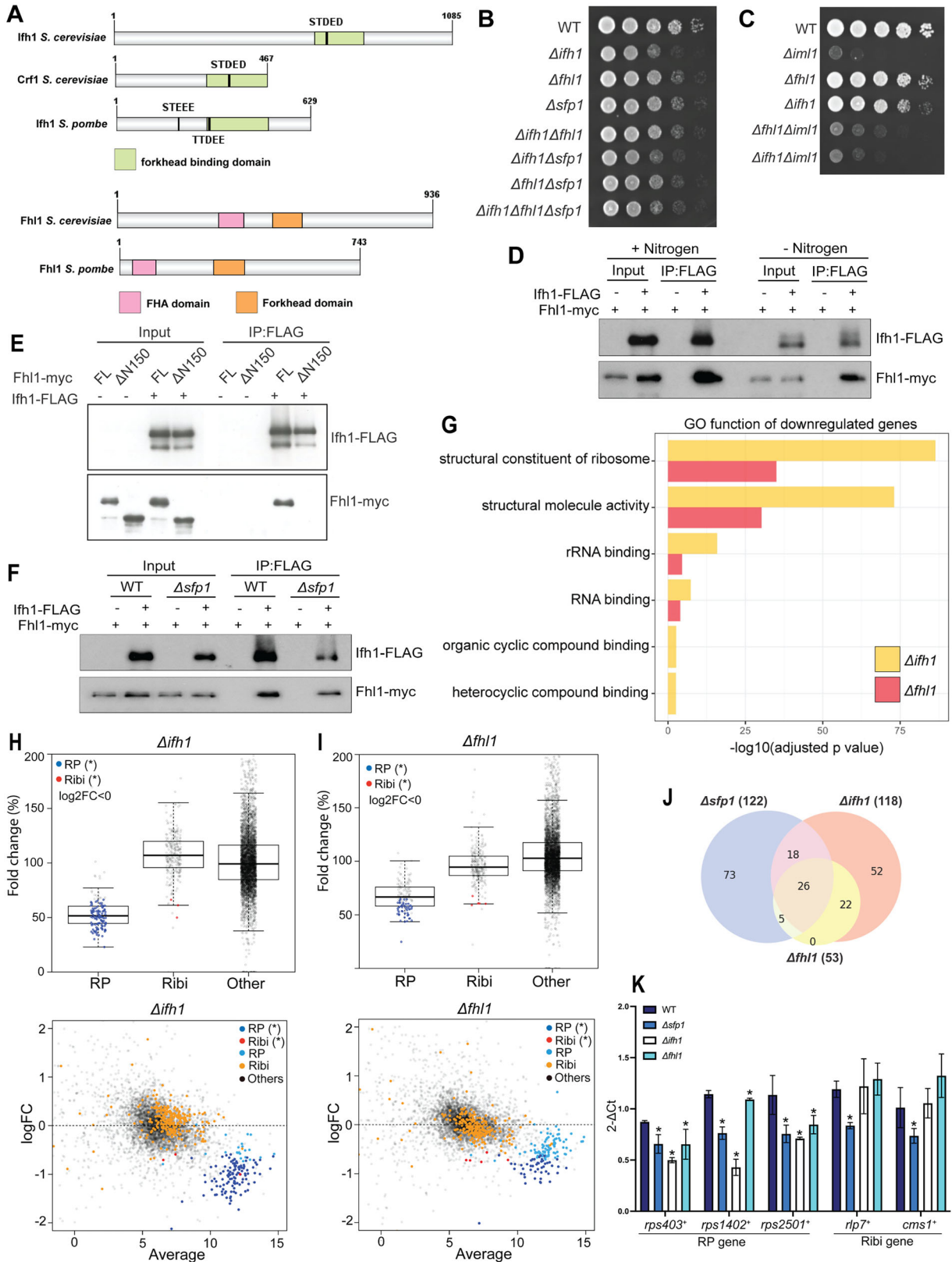


**FIG 4** Sfp1 acts with the Ifh1-Fhl1 complex in the regulation of ribosome production. (A) Comparison of Ifh1/Crf1 and Fhl1 in *S. pombe* and *S. cerevisiae*. The schematic highlights the forkhead binding (green), FHA (pink), and forkhead (orange) domains. CK2-dependent phosphorylation sites in *S. cerevisiae* Ifh1 and Crf1, along with similar sequences identified in *S. pombe* Ifh1, are labeled. (B and C) The indicated strains were spotted in serial dilutions onto solid YES medium. (D–F) The interaction between Ifh1 and Fhl1 was examined by immunoprecipitation. Ifh1 and Fhl1, each tagged with C-terminal FLAG and *myc* tags, respectively, were expressed from their native chromosomal loci in the indicated strains. Anti-FLAG immunoprecipitation was performed,

were downregulated in  $\Delta fh1$ . Based on the GO function enrichment analysis, most of the downregulated genes in the two mutant strains were categorized as the “structural constituent of ribosome” (Fig. 4G), implying that both *lfh1* and *Fhl1* are involved in ribosome production. As *Sfp1* promotes the transcription of the Ribi and RP genes, we checked if *lfh1* and *Fhl1* also regulate these two gene classes. As expected, 81.6% (115 out of 141) of the RP genes and 1% (3 out of 292) of the Ribi genes exhibited downregulation in the  $\Delta ifh1$  mutant (Fig. 4H, Supplementary material, Table S3). Similarly, the  $\Delta fh1$  mutant displayed a reduction in 34% (48 out of 141) of the RP genes and 1.7% (5 out of 292) of the Ribi genes (Fig. 4I and Supplementary material, Table S4), most of which were also downregulated in the  $\Delta ifh1$  mutant (Fig. 4J). The comparison of these gene expression profiles suggests that *lfh1* and *Fhl1* primarily regulate the RP genes whereas *Sfp1* regulates both RP and Ribi genes. This conclusion was further confirmed by the RT-PCR analysis of some representative genes; expression of the Ribi genes *rlp7<sup>+</sup>* and *cms1<sup>+</sup>* was reduced in the  $\Delta sfp1$  mutant but not in the  $\Delta ifh1$  and  $\Delta fh1$  mutants, whereas the transcripts of the RP genes such as *rps403<sup>+</sup>*, *rps1402<sup>+</sup>*, and *rps2501<sup>+</sup>* were reduced in all the three mutants (Fig. 4K). The RNA-seq data collectively suggest that the genes regulated by *lfh1* and *Fhl1* significantly overlap; particularly, these transcription factors appear to play an important role in the expression of the RP genes. Many of those RP genes are also affected by *Sfp1*, although *Sfp1* controls the expression of a number of Ribi genes independently of *lfh1* and *Fhl1*.

**Sfp1, *lfh1*, and *Fhl1* bind to the RP and Ribi genes.** To uncover the target genes of *Sfp1*, *lfh1*, and *Fhl1* in fission yeast, we conducted ChIP-seq (chromatin immunoprecipitation followed by sequencing) experiments using strains expressing these proteins tagged with C-terminal FLAG. Our analysis identified 555, 606, and 577 genes as targets for *Sfp1*, *lfh1*, and *Fhl1*, respectively, with a substantial overlap of 42.9% (351 out of 818) (Fig. 5A). Functional enrichment analysis of the target genes exhibited significant enrichment in GO terms such as structural constituent of ribosome and structural molecule activity, consistent with our RNA-seq results (Fig. 5B). Moreover, 20.1%, 22%, and 14.8% of genes bound by *lfh1*, *Fhl1*, and *Sfp1*, respectively, were RP genes (Fig. 5C). Subsequently, ChIP-qPCR assays were conducted on two representative RP genes, *rps2501<sup>+</sup>* and *rps1402<sup>+</sup>*, confirming the enrichment of *lfh1*, *Fhl1*, and *Sfp1* at these loci (Fig. 5D and E). The binding peaks of these three transcription factors at the RP genes were not confined to their promoter regions (Fig. 5D and E), raising the possibility that those factors are implicated in various aspects of gene expression.

Unlike the RP genes, the Ribi genes account for only a small fraction of the genes bound by *lfh1*, *Fhl1*, and *Sfp1* (3.8%, 4.2%, and 4.3%, respectively) (Fig. 5F). While *Sfp1* impacts the expression of numerous Ribi genes, it is bound to only 8.2% of the total Ribi genes. This was confirmed by ChIP-qPCR assays, where we were unable to detect *Sfp1* binding at *cms1<sup>+</sup>* despite observing a substantial downregulation of this gene in the  $\Delta sfp1$  mutant (Fig. 5G). In contrast, *Sfp1* binding to another Ribi gene, *rlp7<sup>+</sup>*, which exhibited reduced expression upon *Sfp1* deletion, was detectable, and the co-occupancy of *lfh1*, *Fhl1*, and *Sfp1* at this locus was observed (Fig. 5H). Thus, ChIP can detect *Sfp1* binding at a significant portion of the RP genes, but only a small fraction of the Ribi genes.

To examine the role of *lfh1* in the binding of *Sfp1* to its targets, we analyzed *Sfp1* binding to the RP and Ribi genes in the absence of *lfh1*. We observed a significant reduction in the enrichment of *Sfp1* at RP genes, such as *rps2501<sup>+</sup>* and *rps1402<sup>+</sup>*, in the

#### FIG 4 Legend (Continued)

followed by anti-FLAG and anti-*myc* immunoblotting. To assess the function of the FHA domain, full-length (FL) *Fhl1* was compared with a version lacking the N-terminal 150 amino acids ( $\Delta N150$ ) (E). (G) GO functional analysis of genes downregulated in the  $\Delta ifh1$  and  $\Delta fh1$  mutants. The *x* axis (in logarithmic scale) represents adjusted *P* values. Gene ratio is defined as cluster frequency over genome frequency associated with a GO term. (H and I) Box and MA plots illustrating the fold change of the RP and Ribi genes that are downregulated in the  $\Delta ifh1$  (H) and  $\Delta fh1$  (I) mutants. Asterisks indicate a significant difference compared to wild type ( $P < 0.05$ ). (J) Venn diagram depicting the overlap of the downregulated RP and Ribi genes among the  $\Delta ifh1$ ,  $\Delta fh1$ , and  $\Delta sfp1$  mutants. (K) Relative expression levels of representative RP (*rps403<sup>+</sup>*, *rps1402<sup>+</sup>*, and *rps2501<sup>+</sup>*) and Ribi (*rlp7<sup>+</sup>* and *cms1<sup>+</sup>*) genes in the indicated strains, as determined by RT-PCR. Data represent the mean  $\pm$  SD (*n* = 3). Asterisks denote a significant difference relative to wild type ( $P < 0.05$ ).

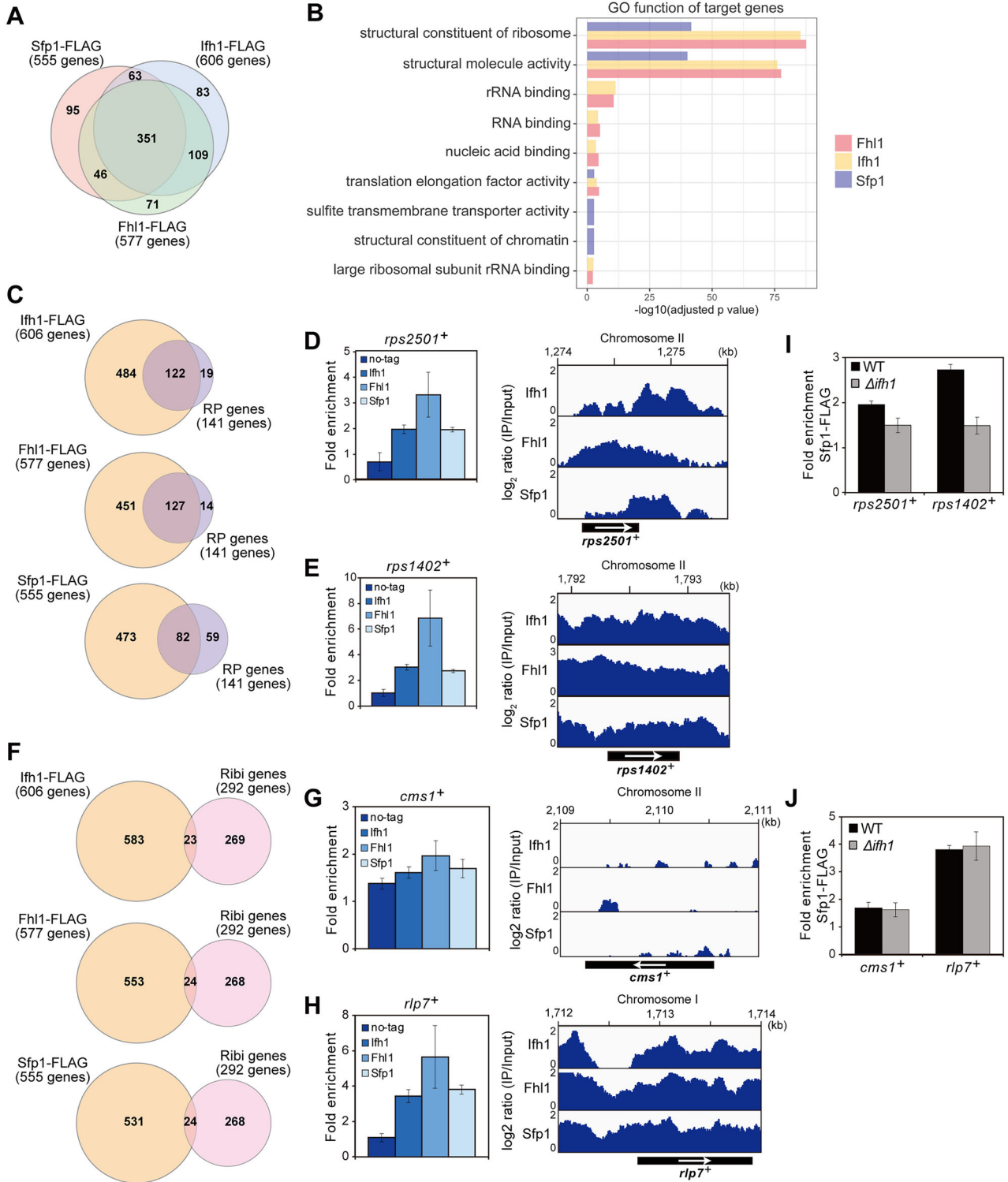


**FIG 5** Sfp1, Ifh1, and Fhl1 bind to the RP and Ribi genes. (A) Venn diagram representing the overlap of ChIP-seq target genes among Sfp1, Ifh1, and Fhl1. (B) GO functional analysis of target genes for Sfp1, Ifh1, and Fhl1. The x axis (in logarithmic scale) represents adjusted P values. (C) Venn diagram representing the overlap between the RP genes and target genes for Ifh1, Fhl1, or Sfp1. (D and E) Bar graphs indicate fold enrichment of Ifh1, Fhl1, and Sfp1 at representative RP genes relative to *prp3*<sup>+</sup> (left). Data represent the mean  $\pm$  SEM (n = 3). IGV tracks depict binding peaks of Ifh1, Fhl1, and Sfp1 at the indicated gene loci (right). Y axes represent log<sub>2</sub> ratio of immunoprecipitation to input (IP/input), and x axes mark chromosome regions. Black boxes represent corresponding genes, with white arrows signifying the direction of transcription. (F) Venn diagram indicating the overlap between the Ribi genes and target genes for Ifh1, Fhl1, or Sfp1. (G and H) Assessment of Ifh1, Fhl1, and Sfp1 binding to representative Ribi genes, conducted as described in (D). (I and J) Fold enrichment of Sfp1 at the indicated gene loci relative to *prp3*<sup>+</sup> in wild-type and  $\Delta$ *ifh1* cells. The data for wild type are the same as those for Sfp1 in (D), (E), (G), and (H). Data represent the mean  $\pm$  SEM (n = 3).

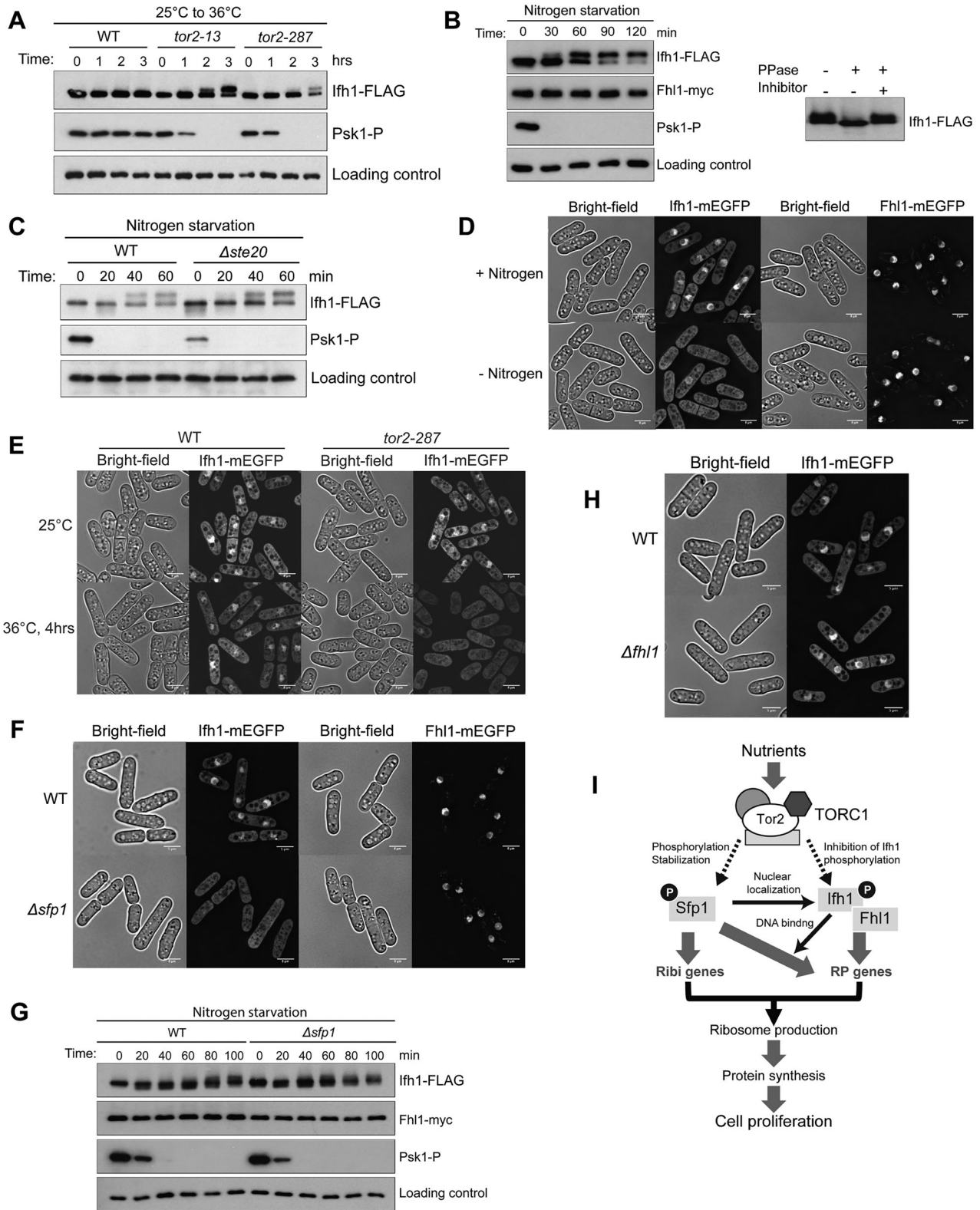


**FIG 6** *lfh1* is under the regulation of TORC1. (A) The indicated strains expressing FLAG-tagged *lfh1* from its native chromosomal locus were cultured in liquid YES medium at 25°C and shifted to 36°C. (B and C) The indicated strains expressing C-terminal FLAG-tagged *lfh1* and *myc*-tagged *Fhl1* from their native chromosomal loci were cultured in liquid EMM medium and then shifted to the same medium lacking nitrogen. Phosphorylation of *lfh1* was verified by lambda phosphatase (PPase) treatment in the presence (+) or absence (-) of phosphatase inhibitors (B). (D-F) The indicated strains expressing mEGFP-tagged *lfh1* or *Fhl1* were analyzed by microscopy. Z axial images were collected and mid-section images after deconvolution are shown. Scale bars, 5  $\mu$ m. (G) The indicated strains were subjected to nitrogen starvation and immunoblotting as in (B). (H) The indicated strains expressing mEGFP-tagged *lfh1* were analyzed as in (F). Scale bars, 5  $\mu$ m. (I) Proposed mechanism of TORC1-mediated control of cell proliferation via Sfp1-regulated ribosome biogenesis.



$\Delta$ *lfh1* mutant (Fig. 5I). In contrast, the interaction of Sfp1 with *rlp7*<sup>+</sup> remained unaffected by the absence of *lfh1* (Fig. 5J), consistent with our finding that *rlp7*<sup>+</sup> expression is independent of *lfh1* (Fig. 4K). These results suggest that *lfh1* facilitates the recruitment of Sfp1 to the RP genes, thereby promoting their expression.

**lfh1 is under the regulation of TORC1.** As *lfh1* and *Fhl1* are involved in the expression of the RP genes that are under the regulation of Sfp1, we examined whether *lfh1* and *Fhl1* are also controlled by TORC1. When TORC1 was inactivated in the *tor2-13* or *tor2-287* mutants at the restrictive temperature, the electrophoretic mobility of *lfh1* was notably decreased (Fig. 6A). The slow migrating form of *lfh1* was also observed when TORC1 was inactivated in wild-type cells starved of nitrogen (Fig. 6B). Phosphatase treatment experiments confirmed that slow-migrating *lfh1* was its phosphorylated form (Fig. 6B). In contrast, the *lfh1* mobility was not affected by the loss of the Ste20 subunit of TORC2 (Fig. 6C), indicating that TORC2 is not involved in the *lfh1* phosphorylation. These data suggest that the phosphorylation status of *lfh1* is under regulation by TORC1.

Remarkably, we discovered that *lfh1* accumulates in the nucleus in a TORC1-dependent manner. In wild-type cells expressing *lfh1* with the fluorescent mEGFP tag, *lfh1* appeared to be concentrated in the nucleus, with some cytoplasmic signals (Fig. 6D). When TORC1 was inactivated by nitrogen starvation (Fig. 6D) or the *tor2-287* mutation (Fig. 6E), the nuclear accumulation of *lfh1* was largely lost while no change in the *lfh1* protein levels was observed (Fig. 6B), implying that TORC1 promotes the nuclear localization of *lfh1*. Moreover, the nuclear signal of *lfh1* was also significantly reduced in the  $\Delta$ *sfp1* mutant (Fig. 6F), though neither the protein level nor the mobility shift of *lfh1* was affected by the  $\Delta$ *sfp1* mutation (Fig. 6G). Therefore, we infer that Sfp1 stabilized by TORC1 promotes the nuclear localization of *lfh1* independently of the phosphorylation state of *lfh1*; inactivation of TORC1 triggers Sfp1 degradation (Fig. 2), which results in the release of *lfh1* from the nucleus. It should also be noted that the nuclear localization of *lfh1* is not dependent on *Fhl1* (Fig. 6H). *Fhl1* was constitutively found in the nucleus, without being affected by TORC1 inactivation (Fig. 6D) or the loss of Sfp1 (Fig. 6F).

These results suggest that the TORC1–Sfp1 pathway regulates the *lfh1* nuclear localization, and together with *Fhl1*, controls the genes involved in ribosome production, promoting cell proliferation in fission yeast (Fig. 6I).

## DISCUSSION

TORC1 promotes the biosynthesis of cellular macromolecules through the phosphorylation of a variety of substrates. As in other eukaryotes, TORC1 in fission yeast is essential for cell viability; the null mutants of the TORC1 components, such as Tor2 and Mip1, and that of the TORC1 activator Rhb1 are lethal.<sup>18,21–23</sup> Nevertheless, the known substrates of TORC1 are apparently dispensable for cell viability,<sup>20,25,41</sup> raising the possibility that there may be additional unknown TORC1 substrate(s) crucial for cell proliferation in fission yeast.

In this study, we have identified the transcription factor Sfp1 in *S. pombe* as a gene product whose overexpression complements the growth defect and rapamycin sensitivity of the TORC1-hypoactive mutants. In addition, the loss of Sfp1 brings about rapamycin sensitivity and can mitigate the TORC1-hyperactive mutants, consistent with the idea that Sfp1 mediates the TORC1 function in promoting cell proliferation. Our data also suggest that nutrient-activated TORC1 phosphorylates and stabilizes the Sfp1 protein by preventing its proteasome-dependent degradation. Collectively, our findings support the notion that Sfp1 is a direct target of TORC1 in fission yeast.

In budding yeast, which is phylogenetically distant from fission yeast, an Sfp1 ortholog promotes cell growth when fermentable glucose is the carbon source.<sup>27,42</sup> Similarly, fission yeast Sfp1 appears to play a significant role in growth control when cells grow on glucose as the carbon source, but not on non-fermentable glycerol (Fig. 1H). In budding yeast, Sfp1 acts as a transcription factor that positively regulates



the RP and Ribi genes and promotes ribosome production.<sup>35,42–45</sup> It is phosphorylated by TORC1, leading to its nuclear localization in a manner regulated by Mrs6, a Rab escort protein whose function remains unclear.<sup>46,47</sup> When TORC1 is inactivated upon starvation, Sfp1 is dephosphorylated and relocated to the cytoplasm, leading to attenuation of ribosome biogenesis.<sup>35,44,46,48</sup> In human cells, an Sfp1 ortholog called juxtaposed with another zinc finger protein 1 (JAZF1) is associated with tumor progression.<sup>49–51</sup> Like yeast Sfp1, JAZF1 promotes ribosome biosynthesis, and its nuclear localization is positively regulated by high glucose.<sup>52</sup> It would be of great interest to investigate whether JAZF1 promotes cell proliferation in response to nutrient availability under the regulation of mTORC1.

Our RNA-seq analyses suggest that fission yeast Sfp1 regulates the RP and Ribi gene transcription. A comprehensive study in budding yeast by ChIP and chromatin endogenous cleavage (ChEC) has found that Sfp1 directly controls many of the RP and Ribi genes as well as other growth-promoting genes.<sup>42</sup> Thus, the role of the Sfp1 transcription factor in the expression of the ribosome biosynthesis genes appears to be conserved between fission yeast and budding yeast. The cellular ribosome content is tightly linked to cellular growth control.<sup>53,54</sup> Upon nitrogen or glucose starvation in fission yeast, TORC1 inactivation allows Sfp1 to be degraded, which may contribute to bringing protein synthesis to a halt through the downregulation of ribosome biosynthesis.

In addition to Sfp1, this study has characterized two additional transcription factors, Fhl1 and Ifh1, which form a complex that plays an important role in the expression of the genes required for ribosome production. Our RNA-seq analyses revealed that Sfp1 regulates both RP and Ribi genes, while the Ifh1-Fhl1 complex primarily contributes to RP gene expression (Figs. 3 and 4). This observation was further confirmed by ChIP-Seq, where the target genes of these three transcription factors were found to be predominantly associated with ribosome biogenesis (Fig. 5B). We successfully verified the co-occupancy of Sfp1, Fhl1, and Ifh1 at the RP genes (Fig. 5D and E). In addition, we encountered a limitation in detecting Sfp1 binding at the Ribi genes (Fig. 5G and H), consistent with previous findings in budding yeast that ChIP was not effective in detecting the binding of Sfp1 at most of the Ribi genes it regulates.<sup>42,55</sup> Therefore, it remains possible that Sfp1 in fission yeast binds to more of the Ribi genes to promote their expression.

Fhl1 and Ifh1 orthologs are present in budding yeast where Fhl1 forms a complex with one of the paralogous transcription coregulators, Ifh1 or Crf1.<sup>36,38,45,56–58</sup> Fhl1 in budding yeast specifically and constitutively resides at the RP gene promoters.<sup>36,59</sup> Under nutrient-rich conditions, the RP gene expression is induced by Fhl1 associated with the Ifh1 coactivator, which is replaced by the Crf1 corepressor under starvation and stress conditions to suppress the RP genes.<sup>36,56–58,60</sup> Fission yeast has only a single Ifh1/Crf1 ortholog that we here call Ifh1, as it appears to serve as an activator, rather than a repressor, of the RP gene expression since our RNA-seq data showed that removal of Ifh1 caused significant downregulation of the RP genes (Fig. 4G–J).

Our findings indicate that in fission yeast, Ifh1 physically interacts with Fhl1 through the FHA domain of Fhl1, similar to the mechanism reported in budding yeast.<sup>57,58</sup> Despite the interaction between Ifh1 and Fhl1, fewer RP genes are downregulated in the  $\Delta fhl1$  mutant compared to the  $\Delta ifh1$  mutant (Fig. 4H and I). Possibly, Sfp1 or other transcription factors may facilitate the association of Ifh1 with the RP genes, as Rap1, Hmo1, and Fpr1 in budding yeast cooperate with Ifh1 in the regulation of ribosome biogenesis.<sup>45,56,58,61</sup>

Ifh1 accumulates in the nucleus only in the presence of ample nitrogen, whereas Fhl1 is constitutively localized in the nucleus (Fig. 6D). The Ifh1-Fhl1 interaction was largely unaffected by the nitrogen availability and hence, we speculate that the basal level of Ifh1 in the nucleus is sufficient to produce the bulk of Ifh1-Fhl1 complex. The nuclear accumulation of Ifh1 is dependent on both TORC1 activity and Sfp1 (Fig. 6D to F). One explanation is that TORC1 indirectly regulates the Ifh1 localization through Sfp1

because Sfp1 is degraded upon TORC1 inactivation (Fig. 2). Therefore, it is possible that Sfp1 or Sfp1-induced gene products interact with Ifh1 and promote the nuclear localization of Ifh1. Alternatively, Sfp1 organizes the chromatin structure that is suitable for the chromatin binding of Ifh1. Indeed, the genetic interaction among Sfp1, Fhl1, and Ifh1 suggests that they function in the same pathway (Fig. 4B). Furthermore, most of the RP genes whose expression is reduced in the  $\Delta sfp1$  mutant are also downregulated in the  $\Delta ifh1$  and  $\Delta fhl1$  mutants. Thus, our findings are consistent with the model that the TORC1 inactivation upon starvation induces the Sfp1 degradation, which delocalizes Ifh1 from the nucleus, leading to a decrease in the Fhl1-Ifh1 complex required for the RP gene expression.

In addition to the nuclear localization, the phosphorylation status of Ifh1 appears to be regulated by TORC1; the phosphorylated, slow-migrating form of Ifh1 was detected when TORC1 is inactivated (Fig. 6A and B). Thus, TORC1 may activate a protein phosphatase that dephosphorylates Ifh1 or inhibit a protein kinase that phosphorylates Ifh1. Identification of such a phosphatase or kinase as well as the role of the Ifh1 phosphorylation is of interest for future studies. The phosphorylation of the budding yeast Crf1 corepressor, which is orthologous to Ifh1 in fission yeast, is also negatively regulated by TORC1.<sup>36</sup> Thus, there might be a conserved mechanism by which TORC1 regulates the Ifh1/Crf1 proteins through modulation of their phosphorylation. It should be, however, noted that budding yeast Crf1 phosphorylated in the absence of TORC1 activity is translocated into the nucleus, in contrast to fission yeast Ifh1 whose nuclear localization is dependent on active TORC1.

Together with earlier studies in budding yeast, our results in fission yeast suggest that the control of ribosome production through the expression of the RP and Ribi genes is one of the key mechanisms by which nutrient-activated TORC1 promotes cell growth and proliferation. Despite the mechanistic differences, the conservation of this cellular function of TORC1 in the distant yeast species points to the possibility that mammalian TORC1 also regulates ribosome biosynthesis to promote cell growth and proliferation in response to nutrient and growth factors. Ribosome synthesis is a complex cellular process that requires proper regulation to balance the supply and demand of protein production for cellular homeostasis. Indeed, dysregulation in ribosome biogenesis is deleterious enough to bring about cancerous cell proliferation and other disorders.<sup>62,63</sup> As an excellent model organism to study TORC1 signaling,<sup>64</sup> fission yeast is expected to be instrumental in attaining a more comprehensive understanding of how TORC1 controls ribosome biogenesis and cell proliferation in eukaryotic cells.

## MATERIALS AND METHODS

**Fission yeast strains and general techniques.** Fission yeast strains used in this study are listed in Table S5 (Supplementary material). Growth media and genetic manipulations for fission yeast have been described previously.<sup>28,65</sup> For mating and sporulation assays, homothallic haploid cells were spotted on SSA sporulation plates, incubated at 25 °C for 48 h, and analyzed by microscopy.<sup>66</sup> Fluorescence microscopy analysis was performed as described previously.<sup>28,65</sup>

**Spot test assay.** Cells were cultured in YES/EMM liquid medium at 30 °C until reaching OD<sub>600</sub> 1.0–2.0 and the spot test assay was performed as described previously.<sup>28,65</sup> For temperature sensitive mutants, the liquid cultures were incubated at 25 °C. Images were captured by the LAS-4000 system (Fujifilm, Japan).

**Multicopy suppressor screen.** We screened an *S. pombe* genomic library in the multicopy vector pAL for plasmids that could suppress the growth defect of *tor2* temperature-sensitive mutants at the restrictive temperature. Plasmids from growing colonies were isolated and reintroduced into the *tor2* mutants to confirm their suppressive effects. Through sequencing the suppressing plasmids, we identified 69 genomic clones from approximately  $6 \times 10^5$  transformants. Among the clones, one was found to contain the *sfp1*<sup>+</sup> gene, which is responsible for the observed suppression.

**Immunoprecipitation, immunoblotting and mobility shift assay.** Immunoprecipitation and immunoblotting analyses were carried out as described previously.<sup>28,65</sup> For mobility shift assay, phosphatase treatment was performed as described previously.<sup>67</sup> The protein samples were resolved by SDS-PAGE, transferred to nitrocellulose, and probed with antibodies as follows: anti-phospho-p70 S6K (Cell Signaling Technology, USA), anti-Spc1,<sup>68</sup> anti-FLAG (M2, Sigma Aldrich, USA), and anti-myc (9E10, Covance, USA; A-14, Santa Cruz Biotechnology, USA).

**In vitro TORC1 kinase assay.** TORC1 kinase assay was performed as described with modifications.<sup>69,70</sup> Cell lysates from Mip1-FLAG-expressing cells were immunoprecipitated with anti-FLAG antibody. The immunoprecipitates were preincubated with substrates (<sup>3</sup>H-methyl-4E-BP1, GST, or GST-Sfp1) at 30 °C

for 5 min. The reaction was initiated by adding [ $\gamma$ - $^{32}$ P]ATP (final concentration of 0.2 mM, 0.2 MBq/reaction), incubated at 30 °C for 30 min, and stopped by adding SDS-PAGE sample buffer, followed by incubation at 65 °C for 5 min. The samples were separated by SDS-PAGE and visualized by staining with GelCode Blue Safe Protein Stain (Thermo Scientific) and autoradiography.

**RNA extraction, real-time PCR, and RNA-sequencing.** Total RNA was extracted from exponentially growing cells with hot acid phenol and glass beads. For RT-PCR, the PrimeScript RT reagent Kit with gDNA Eraser (Takara Bio) was used. The genomic DNA was removed and the samples were then reverse-transcribed according to the manufacturer's protocols. The *act1<sup>+</sup>* gene was used as a control gene for all experiments. The primers using in this study are listed in [Table S6 \(Supplementary material\)](#).

For RNA-seq, the genomic DNA was removed using RQ1 RNase free DNase (Promega) and rRNA was removed using Ribo-zero Gold rRNA removal kit (Epidemiology). The RNA quality and concentration were determined using BioAnalyzer (Agilent) and Qubit (Thermo Fisher). cDNA libraries were prepared using the NEBNext ultra-directional RNA-library for Illumina (#ES74205) and subjected to paired-end sequencing on the Illumina MiSeq platform. The 76 bp paired-end sequences were mapped using Tophat2 default parameter and the FPKM value was calculated using cufflinks2.<sup>71,72</sup>

**RNA-seq data analysis and visualization.** The up- and downregulated genes were determined using the cuffdiff command in cufflinks (<http://cole-trapnell-lab.github.io/cufflinks/cuffdiff/index.html>) with a default value of false discovery rate (0.05) for the threshold.<sup>73</sup> GO categories of the target genes were determined in the *S. pombe* database (<http://www.pombase.org>) using GO Term Finder (<https://go.princeton.edu/cgi-bin/GOTermFinder>).<sup>74</sup> The GO bar plots were generated using R studio using ggplot2 package.<sup>75</sup>

**ChIP and library preparation.** ChIP was performed according to a previously published paper.<sup>76</sup> The primers used in this study are listed in [Table S6 \(Supplementary material\)](#). DNA fragments obtained from ChIP assays were sheared to a uniform size of 300 bp using the Covaris Focused-ultrasonicator S220 (Covaris). These fragments were subsequently used for library preparation with the NEBNext Ultra II DNA Library Prep Kit (NEB) and NEBNext Multiplex Oligos for Illumina (NEB). Deep sequencing was performed by a commercial service (Macrogen) using the HiSeq X platform (2 × 150 bp; Illumina).

**ChIP-seq data analysis.** Adapter sequences were removed from the paired-end reads using the Cutadapt tool,<sup>77</sup> and the resulting reads were mapped to the *S. pombe* genome using Bowtie2.<sup>78</sup> Subsequently, PCR duplicates were eliminated from the generated BAM files using the MarkDuplicates tool from the Picard suite (<http://broadinstitute.github.io/picard/>). Regions bound by Ifh1-FLAG, Fh1-FLAG, and Sfp1-FLAG were identified through peak calling with MACS2 (options: `-no model -ext size 147, q < 0.01` for Ifh1-FLAG and Fh1-FLAG, `q < 0.05` for Sfp1-FLAG).<sup>79</sup> To stringently define binding sites, we considered only the peaks that were consistently identified in three biological replicates for each factor. Genomic regions bound by each factor were identified by intersecting the binding peaks with gene annotations stored in a GFF3 file provided by PomBase (<https://www.pombase.org/>). The BAM file for replication 1 was converted to BigWig format and visualized using the Integrative Genomics Viewer (IGV).<sup>80</sup> The resulting read tracks are presented in this study.

## ACKNOWLEDGEMENTS

We thank M. Uritani and the National Bio-Resource Project (NBRP, Japan) for yeast strains. We also thank the NIBB Radioisotope Center and M. Yamasaki for their technical support.

## AUTHOR CONTRIBUTIONS

YTT: investigation, writing – original draft preparation; TF: conceptualization, investigation, writing – original draft preparation, supervision, funding acquisition; YM: investigation, funding acquisition; HH: investigation; AHO: investigation, funding acquisition; YK: investigation; YA: investigation; TK: resources; KO: resources, funding acquisition; KS: conceptualization, investigation, writing – original draft preparation, supervision, funding acquisition.

## FUNDING

This work was supported by JSPS KAKENHI grant numbers 20K06552 (TF), 23K05679 (TF), 19K06564 (YM), 22K06145 (YM), 19K16070 (AHO), 26291024 (KS), and 19H03224 (KS). This work was also supported by Institute for Fermentation, Osaka (TF and YM), Takeda Science Foundation (TF and KS), Sumitomo Foundation (2200364, YM), JST CREST Grant (JPMJCR1853, KO), AMED Grant (JP20wm0325003 and JP22gm1610007, KO), and Ohsumi Frontier Science Foundation (3-0008, KS).

## ORCID

Tomoyuki Fukuda  <http://orcid.org/0000-0003-2069-7127>

Yoshiaki Kamada  <http://orcid.org/0000-0001-7395-660X>  
 Tomotake Kanki  <http://orcid.org/0000-0001-9646-5379>  
 Kazuhiro Shiozaki  <http://orcid.org/0000-0002-0395-5457>

## DATA AVAILABILITY STATEMENT

The RNA-seq data reported in this article has been deposited in NCBI's Gene Expression Omnibus (GEO) and are accessible through GEO Series accession number GSE201580. The raw data for ChIP-seq analysis have been deposited in the DDBJ database and are publicly accessible under the accession numbers DRA017163, DRA017164, and DRA017165b, associated with BioProject number PRJDB16685.

## DISCLOSURE STATEMENT

No potential conflict of interest was reported by the author(s).

## REFERENCES

- Wullschlegel S, Loewith R, Hall MN. TOR signaling in growth and metabolism. *Cell*. 2006;124:471–484. doi:10.1016/j.cell.2006.01.016.
- Loewith R, Hall MN. Target of rapamycin (TOR) in nutrient signaling and growth control. *Genetics*. 2011;189:1177–1201. doi:10.1534/genetics.111.133363.
- Yang H, Jiang X, Li B, Yang HJ, Miller M, Yang A, Dhar A, Pavletich NP. Mechanisms of mTORC1 activation by RHEB and inhibition by PRAS40. *Nature*. 2017;552:368–373. doi:10.1038/nature25023.
- Inoki K, Li Y, Xu T, Guan K-L. Rheb GTPase is a direct target of TSC2 GAP activity and regulates mTOR signaling. *Genes Dev*. 2003;17:1829–1834. doi:10.1101/gad.1110003.
- Inoki K, Li Y, Zhu T, Wu J, Guan K-L. TSC2 is phosphorylated and inhibited by Akt and suppresses mTOR signalling. *Nat Cell Biol*. 2002;4:648–657. doi:10.1038/ncb839.
- Bar-Peled L, Schweitzer LD, Zoncu R, Sabatini DM. Ragulator is a GEF for the Rag GTPases that signal amino acid levels to mTORC1. *Cell*. 2012;150:1196–1208. doi:10.1016/j.cell.2012.07.032.
- Sancak Y, Bar-Peled L, Zoncu R, Markhard AL, Nada S, Sabatini DM. Ragulator-Rag complex targets mTORC1 to the lysosomal surface and is necessary for its activation by amino acids. *Cell*. 2010;141:290–303. doi:10.1016/j.cell.2010.02.024.
- Sancak Y, Peterson TR, Shaul YD, Lindquist RA, Thoreen CC, Bar-Peled L, Sabatini DM. The Rag GTPases bind raptor and mediate amino acid signaling to mTORC1. *Science*. 2008;320:1496–1501. doi:10.1126/science.1157535.
- Bar-Peled L, Chantranupong L, Cherniack AD, Chen WW, Ottina KA, Grabiner BC, Spear ED, Carter SL, Meyerson M, Sabatini DM. A Tumor suppressor complex with GAP activity for the Rag GTPases that signal amino acid sufficiency to mTORC1. *Science*. 2013;340:1100–1106. doi:10.1126/science.1232044.
- Ben-Sahra I, Manning BD. mTORC1 signaling and the metabolic control of cell growth. *Curr Opin Cell Biol*. 2017;45:72–82. doi:10.1016/j.jceb.2017.02.012.
- Ma XM, Blenis J. Molecular mechanisms of mTOR-mediated translational control. *Nat Rev Mol Cell Biol*. 2009;10:307–318. doi:10.1038/nrm2672.
- Peterson TR, Sengupta SS, Harris TE, Carmack AE, Kang SA, Balderas E, Guertin DA, Madden KL, Carpenter AE, Finck BN, et al. mTOR Complex 1 regulates Lipin 1 localization to control the SREBP pathway. *Cell*. 2011;146:408–420. doi:10.1016/j.cell.2011.06.034.
- Ganley IG, Lam DH, Wang J, Ding X, Chen S, Jiang X. ULK1.ATG13.FIP200 complex mediates mTOR signaling and is essential for autophagy. *J Biol Chem*. 2009;284:12297–12305. doi:10.1074/jbc.M900573200.
- Hosokawa N, Hara T, Kaizuka T, Kishi C, Takamura A, Miura Y, Iemura S, Natsume T, Takehana K, Yamada N, et al. Nutrient-dependent mTORC1 association with the ULK1-Atg13-FIP200 complex required for autophagy. *Mol Biol Cell*. 2009;20:1981–1991. doi:10.1091/mbc.e08-12-1248.
- Kim LC, Cook RS, Chen J. mTORC1 and mTORC2 in cancer and the tumor microenvironment. *Oncogene*. 2017;36:2191–2201. doi:10.1038/ncr.2016.363.
- Fukuda T, Shiozaki K. The Rag GTPase-Ragulator complex attenuates TOR complex 1 signaling in fission yeast. *Autophagy*. 2018;14:1105–1106. doi:10.1080/15548627.2018.1444313.
- Fukuda T, Shiozaki K. Multiplexed suppression of TOR complex 1 induces autophagy during starvation. *Autophagy*. 2021;17:1794–1795. doi:10.1080/15548627.2021.1938915.
- Hayashi T, Hatanaka M, Nagao K, Nakaseko Y, Kanoh J, Kokubu A, Ebe M, Yanagida M. Rapamycin sensitivity of the *Schizosaccharomyces pombe* *tor2* mutant and organization of two highly phosphorylated TOR complexes by specific and common subunits. *Genes Cells*. 2007;12:1357–1370. doi:10.1111/j.1365-2443.2007.01141.x.
- Matsuo T, Otsubo Y, Urano J, Tamanoi F, Yamamoto M. Loss of the TOR kinase Tor2 mimics nitrogen starvation and activates the sexual development pathway in fission yeast. *Mol Cell Biol*. 2007;27:3154–3164. doi:10.1128/MCB.01039-06.
- Otsubo Y, Nakashima A, Yamamoto M, Yamashita A. TORC1-dependent phosphorylation targets in fission yeast. *Biomolecules*. 2017;7:50. doi:10.3390/biom7030050.
- Álvarez B, Moreno S. Fission yeast Tor2 promotes cell growth and represses cell differentiation. *J Cell Sci*. 2006;119:4475–4485. doi:10.1242/jcs.03241.
- Uritani M, Hidaka H, Hotta Y, Ueno M, Ushimaru T, Toda T. Fission yeast Tor2 links nitrogen signals to cell proliferation and acts downstream of the Rheb GTPase. *Genes Cells*. 2006;11:1367–1379. doi:10.1111/j.1365-2443.2006.01025.x.
- Weisman R, Roitburg I, Schonbrun M, Harari R, Kupiec M. Opposite effects of Tor1 and Tor2 on nitrogen starvation responses in fission yeast. *Genetics*. 2007;175:1153–1162. doi:10.1534/genetics.106.064170.
- Nakashima A, Sato T, Tamanoi F. Fission yeast TORC1 regulates phosphorylation of ribosomal S6 proteins in response to nutrients and its activity is inhibited by rapamycin. *J Cell Sci*. 2010;123:777–786. doi:10.1242/jcs.060319.
- Nakashima A, Otsubo Y, Yamashita A, Sato T, Yamamoto M, Tamanoi F. Psk1, an AGC kinase family member in fission yeast, is directly phosphorylated and controlled by TORC1 and functions as S6 kinase. *J Cell Sci*. 2012;125:5840–5849. doi:10.1242/jcs.111146.
- Tanaka K, Yonekawa T, Kawasaki Y, Kai M, Furuya K, Iwasaki M, Murakami H, Yanagida M, Okayama H. Fission yeast Eso1p is required for establishing sister chromatid cohesion during S phase. *Mol Cell Biol*. 2000;20:3459–3469. doi:10.1128/MCB.20.10.3459-3469.2000.
- Cipollina C, Alberghina L, Porro D, Vai M. SFP1 is involved in cell size modulation in respiro-fermentative growth conditions. *Yeast*. 2005;22:385–399. doi:10.1002/yea.1218.
- Chia KH, Fukuda T, Sofyantoro F, Matsuda T, Amari T, Shiozaki K. Ragulator and GATOR1 complexes promote fission yeast growth by attenuating TOR complex 1 through Rag GTPases. *elife*. 2017;6:e30880. doi:10.7554/eLife.30880.
- Kohda TA, Tanaka K, Konomi M, Sato M, Osumi M, Yamamoto M. Fission yeast autophagy induced by nitrogen starvation generates a nitrogen source that drives adaptation processes. *Genes Cells*. 2007;12:155–170. doi:10.1111/j.1365-2443.2007.01041.x.
- Nakashima A, Hasegawa T, Mori S, Ueno M, Tanaka S, Ushimaru T, Sato S, Uritani M. A starvation-specific serine protease gene, *isp6<sup>+</sup>*, is involved in both autophagy and sexual development in *Schizosaccharomyces pombe*. *Curr Genet*. 2006;49:403–413. doi:10.1007/s00294-006-0067-0.



- 31 Marguerat S, Schmidt A, Codlin S, Chen W, Aebersold R, Bähler J. Quantitative analysis of fission yeast transcriptomes and proteomes in proliferating and quiescent cells. *Cell*. 2012;151:671–683. doi:10.1016/j.cell.2012.09.019.
- 32 Gordon C, McGurk G, Wallace M, Hastie ND. A conditional lethal mutant in the fission yeast 26 S protease subunit *mts3<sup>+</sup>* is defective in metaphase to anaphase transition. *J Biol Chem*. 1996;271:5704–5711. doi:10.1074/jbc.271.10.5704.
- 33 Takeda K, Mori A, Yanagida M. Identification of genes affecting the toxicity of anti-cancer drug Bortezomib by genome-wide screening in *S. pombe*. *PLoS One*. 2011;6:e22021. doi:10.1371/journal.pone.0022021.
- 34 Warner JR. The economics of ribosome biosynthesis in yeast. *Trends Biochem Sci*. 1999;24:437–440. doi:10.1016/S0968-0004(99)01460-7.
- 35 Jorgensen P, Rupes I, Sharom JR, Schnepfer L, Broach JR, Tyers M. A dynamic transcriptional network communicates growth potential to ribosome synthesis and critical cell size. *Genes Dev*. 2004;18:2491–2505. doi:10.1101/gad.1228804.
- 36 Martin DE, Soulard A, Hall MN. TOR regulates ribosomal protein gene expression via PKA and the Forkhead transcription factor FHL1. *Cell*. 2004;119:969–979. doi:10.1016/j.cell.2004.11.047.
- 37 Zencir S, Dilg D, Rueda MP, Shore D, Albert B. Mechanisms coordinating ribosomal protein gene transcription in response to stress. *Nucleic Acids Res*. 2020;48:11408–11420. doi:10.1093/nar/gkaa852.
- 38 Wapinski I, Pfiffner J, French C, Socha A, Thompson DA, Regev A. Gene duplication and the evolution of ribosomal protein gene regulation in yeast. *Proc Natl Acad Sci USA*. 2010;107:5505–5510. doi:10.1073/pnas.0911905107.
- 39 Kim MS, Hahn J-S. Role of CK2-dependent phosphorylation of Iyh1 and Crf1 in transcriptional regulation of ribosomal protein genes in *Saccharomyces cerevisiae*. *Biochim Biophys Acta*. 2016;1859:1004–1013. doi:10.1016/j.bbagr.2016.06.003.
- 40 Pataki E, Weisman R, Sipiczki M, Miklos I. *fhl1* gene of the fission yeast regulates transcription of meiotic genes and nitrogen starvation response, downstream of the TORC1 pathway. *Curr Genet*. 2017;63:91–101. doi:10.1007/s00294-016-0607-1.
- 41 Shetty M, Noguchi C, Wilson S, Martinez E, Shiozaki K, Sell C, Mell JC, Noguchi E. Maf1-dependent transcriptional regulation of tRNAs prevents genomic instability and is associated with extended lifespan. *Aging Cell*. 2020;19:e13068. doi:10.1111/acer.13068.
- 42 Albert B, Tomassetti S, Gloor Y, Dilg D, Mattarocci S, Kubik S, Hafner L, Shore D. Sfp1 regulates transcriptional networks driving cell growth and division through multiple promoter-binding modes. *Genes Dev*. 2019;33:288–293. doi:10.1101/gad.322040.118.
- 43 Fingerman I, Nagaraj V, Norris D, Vershon AK. Sfp1 plays a key role in yeast ribosome biogenesis. *Eukaryot Cell*. 2003;2:1061–1068. doi:10.1128/EC.2.5.1061-1068.2003.
- 44 Marion RM, Regev A, Segal E, Barash Y, Koller D, Friedman N, O’Shea EK. Sfp1 is a stress- and nutrient-sensitive regulator of ribosomal protein gene expression. *Proc Natl Acad Sci USA*. 2004;101:14315–14322. doi:10.1073/pnas.0405353101.
- 45 Hirai H, Ohta K. Comparative research: regulatory mechanisms of ribosomal gene transcription in *Saccharomyces cerevisiae* and *Schizosaccharomyces pombe*. *Biomolecules*. 2023;13:288. doi:10.3390/biom13020288.
- 46 Lempiäinen H, Uotila A, Urban J, Dohnal I, Ammerer G, Loewith R, Shore D. Sfp1 interaction with TORC1 and Mrs6 reveals feedback regulation on TOR signaling. *Mol Cell*. 2009;33:704–716. doi:10.1016/j.molcel.2009.01.034.
- 47 Singh J, Tyers M. A Rab escort protein integrates the secretion system with TOR signaling and ribosome biogenesis. *Genes Dev*. 2009;23:1944–1958. doi:10.1101/gad.1804409.
- 48 Jorgensen P, Nishikawa JL, Breitkreutz B-J, Tyers M. Systematic identification of pathways that couple cell growth and division in yeast. *Science*. 2002;297:395–400. doi:10.1126/science.1070850.
- 49 Zhou D-z, Liu Y, Zhang D, Liu S-m, Yu L, Yang Y-f, Zhao T, Chen Z, Kan M-y, Zhang Z-f, et al. Variations in/nearby genes coding for JAZF1, TSPAN8/LGR5 and HHEX-IDE and risk of type 2 diabetes in Han Chinese. *J Hum Genet*. 2010;55:810–815. doi:10.1038/jhg.2010.117.
- 50 Alharbi KK, Ali Khan I, Syed R, Alharbi FK, Mohammed AK, Vinodson B, Al-Daghri NM. Association of JAZF1 and TSPAN8/LGR5 variants in relation to type 2 diabetes mellitus in a Saudi population. *Diabetol Metab Syndr*. 2015;7:92. doi:10.1186/s13098-015-0091-7.
- 51 Sung Y, Park S, Park SJ, Jeong J, Choi M, Lee J, Kwon W, Jang S, Lee M-H, Kim DJ, et al. Jazf1 promotes prostate cancer progression by activating JNK/Slug. *Oncotarget*. 2018;9:755–765. doi:10.18632/oncotarget.23146.
- 52 Kobiita A, Godbersen S, Araldi E, Ghoshdastider U, Schmid MW, Spinas G, Moch H, Stoffel M. The diabetes gene JAZF1 is essential for the homeostatic control of ribosome biogenesis and function in metabolic stress. *Cell Rep*. 2020;32:107846. doi:10.1016/j.celrep.2020.107846.
- 53 Dai X, Zhu M. Coupling of ribosome synthesis and translational capacity with cell growth. *Trends Biochem Sci*. 2020;45:681–692. doi:10.1016/j.tibs.2020.04.010.
- 54 Kelly SP, Bedwell DM. Both the autophagy and proteasomal pathways facilitate the Ubp3p-dependent depletion of a subset of translation and RNA turnover factors during nitrogen starvation in *Saccharomyces cerevisiae*. *RNA*. 2015;21:898–910. doi:10.1261/rna.045211.114.
- 55 Reja R, Vinayachandran V, Ghosh S, Pugh BF. Molecular mechanisms of ribosomal protein gene coregulation. *Genes Dev*. 2015;29:1942–1954. doi:10.1101/gad.268896.115.
- 56 Schawalder S, Kabani M, Howald I, Choudhury U, Werner M, Shore D. Growth-regulated recruitment of the essential yeast ribosomal protein gene activator Iyh1. *Nature*. 2004;432:1058–1061. doi:10.1038/nature03200.
- 57 Rudra D, Zhao Y, Warner JR. Central role of Iyh1p–Fhl1p interaction in the synthesis of yeast ribosomal proteins. *EMBO J*. 2005;24:533–542. doi:10.1038/sj.emboj.7600553.
- 58 Wade J, Hall D, Struhl K. The transcription factor Iyh1 is a key regulator of yeast ribosomal protein genes. *Nature*. 2004;432:1054–1058. doi:10.1038/nature03175.
- 59 Lee TI, Rinaldi NJ, Robert F, Odom DT, Bar-Joseph Z, Gerber GK, Hannett NM, Harbison CT, Thompson CM, Simon I, et al. Transcriptional regulatory networks in *Saccharomyces cerevisiae*. *Science*. 2002;298:799–804. doi:10.1126/science.1075090.
- 60 Albert B, Kos-Braun IC, Henras AK, Dez C, Rueda MP, Zhang X, Gadal O, Kos M, Shore D. A ribosome assembly stress response regulates transcription to maintain proteome homeostasis. *Elife*. 2019;8:e45002. doi:10.7554/eLife.45002.
- 61 Kasahara K, Nakayama R, Shiwa Y, Kanesaki Y, Ishige T, Yoshikawa H, Kokubo T. Fpr1, a primary target of rapamycin, functions as a transcription factor for ribosomal protein genes cooperatively with Hmo1 in *Saccharomyces cerevisiae*. *PLoS Genet*. 2020;16:e1008865. doi:10.1371/journal.pgen.1008865.
- 62 Freed EF, Bleichert F, Dutca LM, Baserga SJ. When ribosomes go bad: diseases of ribosome biogenesis. *Mol Biosyst*. 2010;6:481–493. doi:10.1039/b919670f.
- 63 Pelletier J, Thomas G, Volarević S. Ribosome biogenesis in cancer: new players and therapeutic avenues. *Nat Rev Cancer*. 2018;18:51–63. doi:10.1038/nrc.2017.104.
- 64 Morozumi Y, Shiozaki K. Conserved and divergent mechanisms that control TORC1 in yeasts and mammals. *Genes (Basel)*. 2021;12:88. doi:10.3390/genes12010088.
- 65 Fukuda T, Sofyantoro F, Tai YT, Chia KH, Matsuda T, Murase T, Morozumi Y, Tatebe H, Kanki T, Shiozaki K. Tripartite suppression of fission yeast TORC1 signaling by the GATOR1–Sea3 complex, the TSC complex, and Gcn2 kinase. *Elife*. 2021;10:e60969. doi:10.7554/eLife.60969.
- 66 Kunitomo H, Sugimoto A, Wilkinson C, Yamamoto M. *Schizosaccharomyces pombe pac2<sup>+</sup>* controls the onset of sexual development via a pathway independent of the cAMP cascade. *Curr Genet*. 1995;28:32–38. doi:10.1007/BF00311879.
- 67 Morigasaki S, Chin LC, Hatano T, Emori M, Iwamoto M, Tatebe H, Shiozaki K. Modulation of TOR complex 2 signaling by the stress-activated MAPK pathway in fission yeast. *J Cell Sci*. 2019;132:jcs236133. doi:10.1242/jcs.236133.
- 68 Tatebe H, Shiozaki K. Identification of Cdc37 as a novel regulator of the stress-responsive mitogen-activated protein kinase. *Mol Cell Biol*. 2003;23:5132–5142. doi:10.1128/MCB.23.15.5132-5142.2003.
- 69 Kamada Y, Ando R, Izawa S, Matsuura A. Yeast Tor complex 1 phosphorylates eIF4E-binding protein, Caf20. *Genes Cells*. 2023;28:789–799. doi:10.1111/gtc.13067.
- 70 Otsubo Y, Yamashita A, Ohno H, Yamamoto M. *S. pombe* TORC1 activates the ubiquitin-proteasomal degradation of the meiotic regulator Mei2 in cooperation with Pat1 kinase. *J Cell Sci*. 2014;127:2639–2646. doi:10.1242/jcs.135517.
- 71 Kim D, Pertea G, Trapnell C, Pimentel H, Kelley R, Salzberg SL. TopHat2: Accurate alignment of transcriptomes in the presence of insertions, deletions and gene fusions. *Genome Biol*. 2013;14:R36. doi:10.1186/gb-2013-14-4-r36.



- 72 Roberts A, Trapnell C, Donaghey J, Rinn JL, Pachter L. Improving RNA-Seq expression estimates by correcting for fragment bias. *Genome Biol.* 2011;12:R22. doi:10.1186/gb-2011-12-3-r22.
- 73 Trapnell C, Williams BA, Pertea G, Mortazavi A, Kwan G, Van Baren MJ, Salzberg SL, Wold BJ, Pachter L. Transcript assembly and quantification by RNA-Seq reveals unannotated transcripts and isoform switching during cell differentiation. *Nat Biotechnol.* 2010;28:511–515. doi:10.1038/nbt.1621.
- 74 Harris MA, Rutherford KM, Hayles J, Lock A, Bähler J, Oliver SG, Mata J, Wood V. Fission stories: using PomBase to understand *Schizosaccharomyces pombe* biology. *Genetics.* 2022;220:iyab222. doi:10.1093/genetics/iyab222.
- 75 Wickham H. *ggplot2: elegant graphics for data analysis.* New York (NY): Springer-Verlag; 2016. doi:10.1007/978-3-319-24277-4.
- 76 Hirai H, Takemata N, Tamura M, Ohta K. Facultative heterochromatin formation in rDNA is essential for cell survival during nutritional starvation. *Nucleic Acids Res.* 2022;50:3727–3744. doi:10.1093/nar/gkac175.
- 77 Martin M. Cutadapt removes adapter sequences from high-throughput sequencing reads. *EMBnet J.* 2011;17:10–12. doi:10.14806/ej.17.1.200.
- 78 Langmead B, Salzberg SL. Fast gapped-read alignment with Bowtie 2. *Nat Methods.* 2012;9:357–359. doi:10.1038/nmeth.1923.
- 79 Zhang Y, Liu T, Meyer CA, Eeckhoutte J, Johnson DS, Bernstein BE, Nusbaum C, Myers RM, Brown M, Li W, et al. Model-based analysis of ChIP-Seq (MACS). *Genome Biol.* 2008;9:R137. doi:10.1186/gb-2008-9-9-r137.
- 80 Robinson JT, Thorvaldsdóttir H, Winckler W, Guttman M, Lander ES, Getz G, Mesirov JP. Integrative genomics viewer. *Nat Biotechnol.* 2011;29:24–26. doi:10.1038/nbt.1754.